3

Evaluation of Synergistic Effect of Plant Extracts for Cathodic Inhibition of Steel in Acidic Media

*Sodiya E. F. and Aladesuyi O.

Department of Chemical sciences,
Mountain Top University, Ibafo, Nigeria

Department of Industrial Chemistry,
Covenant University, Ota, Nigeria

*Corresponding author e-mail: efsodiya@mtu.edu.ng

Abstract

The synergistic effect of combining both Sida acuta (SA) and Jatropha curcas (JC) leaf extracts on steel in 1.0 M HCl solution was investigated using gasometric and conventional weight loss technique at 30 $^{\circ}$C and 50 $^{\circ}$C. Surface microscture of the steel with the mixed extract were studied through Scanning electron microscope (SEM) and Electron dispersive X-ray spectroscopy (EDX) which revealed how the inhibitor hindered the attack of acid on the microstructures thereby preventing its dissolution into the corrodent. The presence of C=O functional band at 1094 cm^{-1} of ester was confirmed by Fourier transform infrared analysis. Synergism Parameter (S1) was at optimum at 2.09 and 2.65 at 30 $^{\circ}$C and 50 $^{\circ}$C respectively on steel pipe. This implies that synergism is favoured with increase in temperature. S1 greater than 1 confirmed that the mixture of the two plants produced synergised inhibitive effect. The inhibitory power increases with increase in extract concentration. Inhibition Efficiency ranges from 60 % to 85 % with increase in extract concentration of SA alone from 0.1 gdm^{-3} to 1.0 gdm^{-3}. When synergised with JC, it ranges from 77 % to 93 % for SA at 30 $^{\circ}$C for the same concentration increase. Results obtained showed that the synergetic effects of the plants extract complimented carbon constituent of the steel to enhanced the corrosion inhibition potential synergized plant extracts over unsynergized on the steel.

Keywords: Synergism, *Jatropha curcas, Sida acuta,* Cathodic, Corrosion inhibition

1.0 Introduction

Steel have been of immense important in the world of constructions and therefore required much work to be expended on it for preservation from corrosion (Kumari *et al*., 2020; Singh and Quraishi, 2012). Corrosive attack on the pipe occurs from external sources most especially when subjected to highly oxygenated environments such as air water and soil, in particular those containing appreciable acidity content. Plants containing naturally occurring chemical compounds such as tannins, alkaloids, saponins, flavonoids, amino acids and azo dyes detected to possess inhibitory properties, (Oguzie, 2006; Ajanaku *et al*., 2014). Researches made on plant extracts revealed that they are easily accessible, affordable and of less or no harm to human being. This has however made this area to be of high interest and attracts lots of attention. (Ating *et al*., 2010). The use of diverse plant extracts have been found to be good and effective corrosion inhibitors *Occimum Viridis* (Oguzie, 2006), *Nypa Fruticans Wurmb* (Orubite and Oforka, 2004) *Chromolaena Odorata* park extract (Omotosho *et al.,* 2012) *Aningeria Robusta* (Obot *et al*., 2011); *Cola Acuminate* (Ajayi *et al.,* 2011) to mention just a few.

In the quest to improve on the efficacy of inhibitors and also to solve environmental and toxicity associated with chemical inhibitors, synergism of

synthetic inhibitors has been reported (Ita and Offong, 2000; Zhao *et al*., 2015). Little attention has so far been given to synergism of plant extract with each other. Synergism of corrosion inhibitors is either due to interaction between components of the inhibitors (extract and synergistic ions) or due to interaction between the inhibitors and one of the ions present in aqueous solution (H^+, OH^-, SO_4^{2-}, Cl^-) (Umoren *et al.*, 2008). The aim of this present investigation is to study the cathodic protection characteristics of *Sida acuta* synergised with *Jatropha curcas* as alternative corrosion inhibition of steel pipe over galvanisation in acid environments.

2.0 Experimental
2.1 Coupons preparation

Mild steel sheet of 3 mm was sliced with lathe machine into coupons of 18.0 mm x 9.0 mm. The dimensions of these coupons were taken with Mitutoyo digital vernier gauge. Surface of the coupons were degreased in ethanol and dried with acetone. They were thereafter stored in desiccators avoid contamination by moisture prior to use.

2.2 Extraction from Plant

Fresh *Jatropha curcas* (JC) and *Sida acuta* (SA) leaves were air dried and ground into powder. 10 g sample was measured into 250 ml volume conical flask containing 100 mL of ethanol. 5 g each of the plant leaves were weighed and mixed in 250 ml conical flask containing 100 mL ethanol. The flasks were cork sealed and left to remain for 48 hours with intermittent shakings. The resultant mixture was filtered and residue thoroughly washed with ethanol into filtrate. The residue (husk) was re-soaked in 100 ml ethanol for 24 hours. The mixtures were filtered and both filtrates added. The extract was concentrated by ethanol evaporation at 75 °C in rotary evaporator to sticky solid.

2.3 Preparation of stock solution and various concentrations of *Sida acuta* plant extracts

1 g of extract was dissolved in 1.0 litre of 1.0 M HCl to make 1.0 gdm^{-3} of the extract solution. From that further dilutions were made to obtain 0.l gdm^{-3}, 0.35 gdm^{-3}, 0.6 gdm^{-3} and 0.85 gdm^{-3} concentrations. Distilled water was used for the preparation of all solutions from reagents of BDH Chemicals, England Analar grade brand.

2.4 Gasometric analysis

50 mL of 1.0M HCl solution (control) was introduced into Mylius Cell as shown in Fig 1. The coupon was dropped into the corrodent and corked airtight. The hydrogen gas evolved by download displacement of water was recorded on the calibrated tube (inverted burette). Readings were taken at every 1-minute interval for 20 minutes at 30 °C. The experiment was repeated at 50 °C using another coupon but the same

concentration. The experiment was repeated for set of extract concentrations of *S. acuta* and later mixed *J. curcas* in volume ratio 4:1. At the end of each experiment of Hydrogen gas Evolution (HE), the coupon was withdrawn from the tested solution, washed thoroughly with water followed by acetone and dried with air (Mamatha, 2011).

The corrosion rate was calculated by using polynomial regression analysis of the volume of H_2 gas evolved against time by differentiating the equation (Ajayi *et al;* 2011):

$$V = c + bt + at^2 \qquad (1)$$

$$R = \frac{dv}{dt} = b + 2at \qquad (2)$$

$$R = 2at \pm b \qquad (3)$$

By adaptation of equations (1) and (3) in relation to Volume-Time analysis for various concentrations. For example, the measurement of steel in synergized SA with JC relating to 1.0 gdm^{-3} concentration , the corrosion rate in the form of mathematical expression obtained by correlation analysis of volume discharged with time from which polynomial regression analysis of the volume of Hydrogen gas evolved against time was obtained and indicated in equation (4) thus:

$$0.002t^2 + 109t - 0.271 \qquad (4)$$

On differentiating eq. (4) above, we have:
dv/dt $= 2(0.002t) + 0.109$
$= 0.004t + 0.109$, where t = time

The Inhibition Efficiency (I.E %) of the plant extracts was calculated as follows (Ajayi *et al*., 2011):

$$I.E\% = \{1 - (V_{in} / V_{uni})\} \times 100 \qquad (5)$$

Where V_{in} = Volume of hydrogen gas discharged at time t for inhibited solution, V_{uni} = Volume of hydrogen gas discharged at time t for uninhibited solution

$$\theta = \frac{I.E}{100} \qquad (6)$$

Where θ is the surfaced coverage and I.E. = inhibition efficiency

Experimental Setup (Gasometric method)

1 Acid Medium
2 Metal Coupon (zinc)
3 Calibrated Burrette
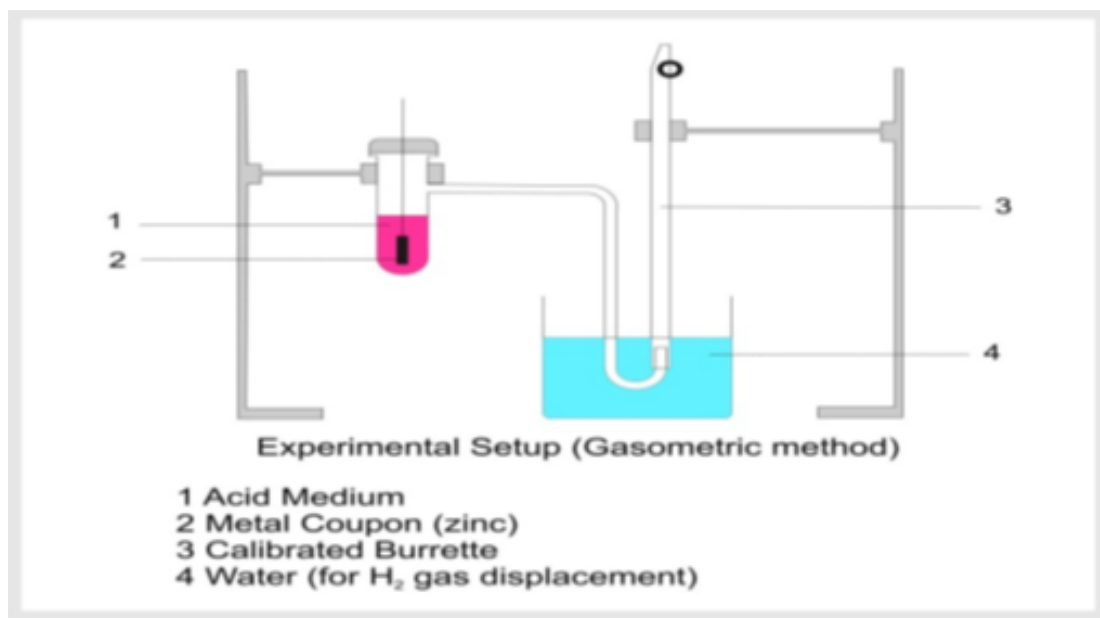4 Water (for H_2 gas displacement)

Fig. 1: Schematic set up of the Gas evolution measurement (Aladesuyi *et al.*, 2018)

2.5 Weight Loss Measurement

The Weight Loss determination was done in line with the method reported in literature (Ating *et al.*, 2010; Ajanaku *et al.*, 2014; Sodiya *et al.*, 2016). The corrodent solution of 100 mL was used. The coupons were dipped in the corrodent and then in corrodent inhibitor containing concentrations of $10 – 50\%$ v/v. 24 hrs intervals were considered for 5 runs. At end of each series the coupons were decanted, treated with washing agent (zinc dust and sodium hydroxide pellet) to stop the effect of the acid HCl and water. It was then dropped in acetone. The weights of the dried corroded coupons were accurately determined with a weighing balance to ascertain the new weight. The Rate of Corrosion (W) and the Percentage Inhibition efficiency I.E. (%) were calculated using equations (7) and (8) (Ating *et al.*, 2010):

$$W = \frac{W_L}{A \times T} \qquad (7)$$

$$I.E.(\%) = \frac{\Delta W_o - \Delta W_{inh}}{\Delta W_o} \times 100 \qquad (8)$$

Where W_L = Initial weight of coupon - Final weight (after coupon withdrawal from solutions)

A = Surface Area of the alloy

T = Time of immersion.

ΔW_o = Change in weight in corrodent (without the inhibitor)

ΔW_{inh} = Change in weight in the presence of inhibitor.

2.6 Deductions from Synergisms

Evaluations were made through this relationship to obtain Synergism Parameter S_1

$$S_1 = \frac{1 - I_{1+2}}{1 - I'_{1+2}} \tag{9}$$

Where $I_{1+2} = I_1 + I_2$

I_1 = Inhibition Efficiency of *Jatropha curcas* extract

I_2 = Inhibition Efficiency of *Sida acuta* extract

I'_{1+2} = Inhibition efficiency of JC and SA combined

2.6 Degree of Interactions between the Synergized Compounds

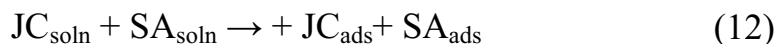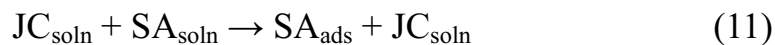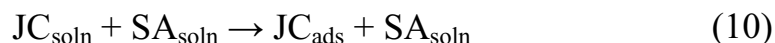$S_1 \rightarrow 1$ = when there are no interactions between the inhibitors (the Synergistic compounds)

$S_1 \cdot 1$ = tending towards synergistic effect

$S_1 < 1$ = indicates antagonistic interaction between the inhibitor compounds (JC and SA) which may be attributed to competitive adsorption to the metal surface or formation of new soluble compounds due to reactions between the two compounds before adsorption process takes place (Aramaki and Hackerman, 1969).

2.7 Synergized Solution of JC and SA

In the solution containing JC and SA, there may be three possible adsorption mechanisms. JC may adsorb before SA, SA may adsorb before JC, JC and SA mixed up due to mixing of secondary metabolites present in both extracts to assume a single compound. These three adsorption mechanisms are described in the equations below (Fishtik *et al.*, 1984):

$$JC_{soln} + SA_{soln} \rightarrow JC_{ads} + SA_{soln} \tag{10}$$

$$JC_{soln} + SA_{soln} \rightarrow SA_{ads} + JC_{soln} \tag{11}$$

$$JC_{soln} + SA_{soln} \rightarrow + JC_{ads} + SA_{ads} \tag{12}$$

3.0   Result and Discussion
3.1   Inhibition Efficiency of the Extract on the Metal

Hydrogen gas evolved by the control (acid containing no extract) is higher than those containing extracts at various concentrations at 30 °C as depicted in Fig. 2. The hydrogen gas evolution is inversely proportional to extract concentrations. The same trend was recorded for the experiment at 50 °C.
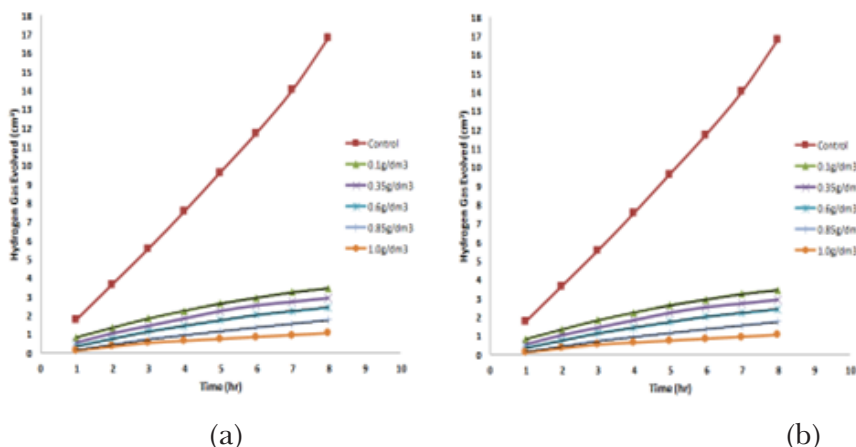

| (a) | (b) |

Fig. 2: Plot of Hydrogen gas discharged (cm³) at various Time (hr) intervals for steel in synergized JC and SA extracts in the presence of 1.0 M HCl at (a) 30 °C and (b) 50 °C

Inhibition Efficiency is directly proportional to extract concentration. At 7th hour, the Inhibition Efficiency increases from 77 % to 93 % at extract concentration of 0.1 gdm⁻³ to 1.0 gdm⁻³ as shown in Fig. 3.   Also at 50 °C, the inhibition efficiency increases with increase in extract concentration from 57 % to 79 % as depicted in Fig. 3 when compared with corresponding time at 30 °C.
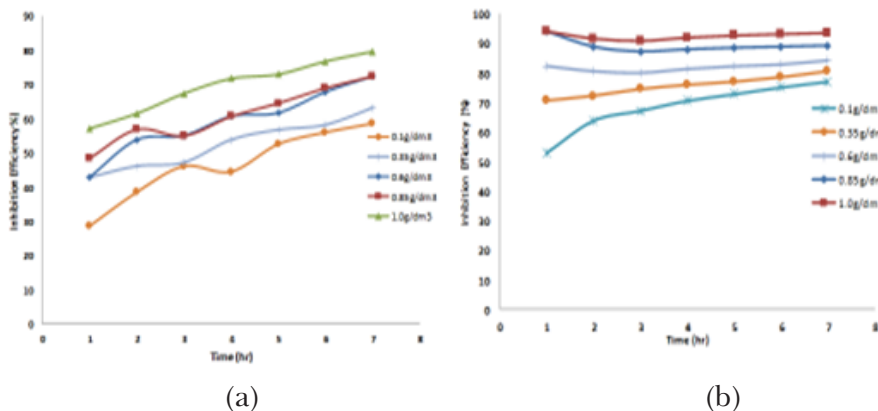

| (a) | (b) |

Fig. 3: Plot of inhibition efficiency (%) with time (hr) for steel synergized JC and SA extracts in the presence of 1.0 M HCl at (a) 30 °C and (b) 50 °C

The corrosion rate of acid solution (control) without extract is exceptional high, but the corrosion rate of extract containng solutions decrease with extract concentrations at 30 °C except for 0.35 gdm⁻³ and 1.0 gdm⁻³ that slightly decreases with time. At 50 °C, corrosion
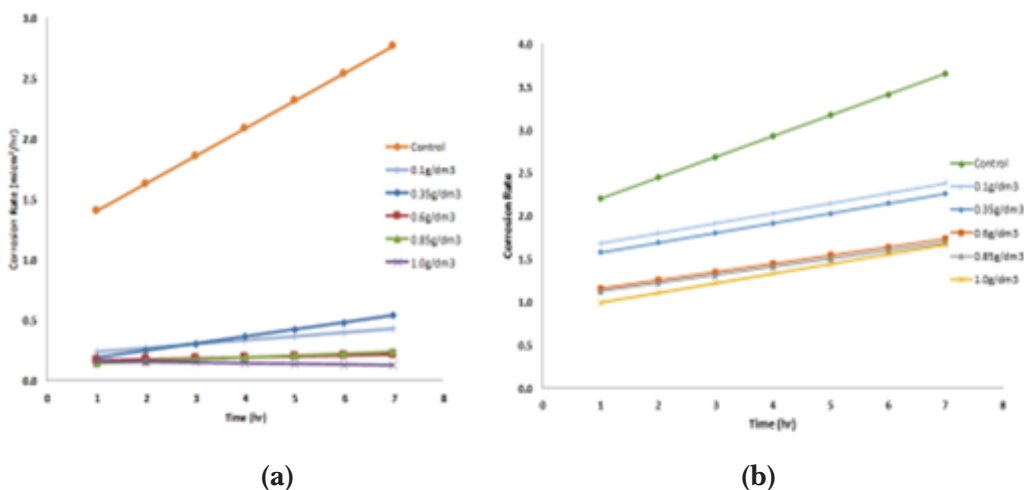

(a)   (b)

Fig. 4: Plot of corrosion rate (mlcm^2/hr) of varying volume dilution ratios of synergized JC and SA extracts with time intervals (hr) for steel corrosion extracts in

3.2 Extract Synergistic Effect on Steel Inhibition

At 30 °C, Synergistic effect S_1 increases from 2.04 at 0.1 gdm⁻³ to 2.09 at 0.6 gdm⁻³ before decreasing to 1.94 at 0.8 gdm⁻³. The Optimum synergy of S_1 2.09 was achieved at extract concentration solution 0.6gdm⁻³. The Inhibition Efficiency (I.E) performance obtained from corrosion inhibition using extract of SA and mixture of SA and JC compared for concentration range of 0.1 to 1.0 gdm⁻³ on steel.

Table 1: Comparison of Synergised and Unsynergized plant extract potency

Temperature	Time	% I.E. SA	% I.E. SA+JC Synergized
30 °C	7th hour:	60 % to 85 %	: 77 % to 93 %
50 °C	7th hour:	56 % to 74 %	: 57 % to 79 %

There was increase in both inhibiting potency as both plant extracts increased with concentrations. Synergy effectiveness confirmed with improved Inhibition efficiency of synergized over unsynergized plant extracts. Reduction in I.E.,% @ 50 °C was due to increase in temperature which lead to desorption. The concentration of 8 gdm^{-3} of JC at constant volume of 10 mL synergized with constant volume of 40 mL (4:1) of 0.1 gdm^{-3} to 1.0 gdm^{-3} SA gave an average improvement of 10 % Inhibition efficiency This is comparable to the report of Umoren et al (2008) that KI of 0.06 M kept constant synergized with Polyvinyl pyrrolidone (PVP) concentration from 2×10^{-5} M to 1×10^{-4} M gave I.E. 13.13 % to 26.26 % at 50 °C. It should be noted that the volume ratio of mixing the two compound KI and PVP was not stipulated as 0.06 M KI equivalent to 9.6gdm^{-3} KI was used to synergize a low concentration of PVP earlier indicated compared with 8 gdm^{-3} of JC in 0.1 gdm^{-3} to 1.0 gdm^{-3} of SA. Also synergistic inhibitive effective effect of KI with the extract of Telfaira occidentalis in 1.0 M HCl by Nwabenne et al., (2011) reported increase in I.E from 44.3 % to 52.3 % due to synergism effect of Iodide ions from KI.
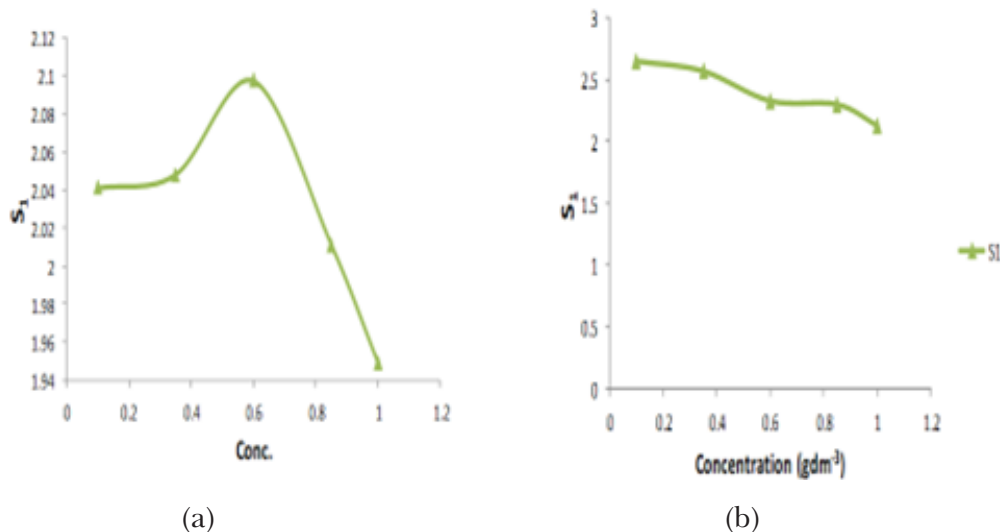

(a)   (b)

Fig. 5: Graphs of Sygnergism S1 against various extract concentrations of steel at (a) 30 °C and (b) 50 °C.

3.3 Heteroatoms Constituents in the Extracts

FTIR analysis confirmed the presence of functional groups in the leaf extract component contained as heteroatoms. The spectrum of *Sida acuta* extract is as shown in Fig. 6 with Table 2 for interpretation. *Jatropha curcas* extract spectrum in Fig. 7 interpreted on Table 3. The spectrum of mixed *Jatropha curcas* with *Sida acuta* plant leave extracts in Fig 8 interpreted on Table 4. The resultant mixture of plant extracts which has been reported to have individually inhibited corrosion of metal performed similar role as in the case of halides in which its addition to plant extracts and some other chemical inhibitors reported to improve inhibition of corrosion on metals. But on the other hand, the addition of plant extract to some solid minerals may induce corrosion which on their own inhibits corrosion of metals (Sodiya *et al.,* 2017). The fact that the leaf extract contains various phyto-constituents and nature of conjugated bonds, corrosion inhibition in this case could not be traced to particular specie out of lots present in the extract. In as much as most of these constituents such as tannins, organic and amino acids, alkaloids, proteins, flavonoids, and organic pigments and their acid hydrolysis products are known to exhibit inhibiting action, this however made it difficult to assign the inhibitive effect by adsorption to a particular constituent (Kliskic *et al*., 2000). In view of these inhibiting effects of extracts of some plant origin have been attributed to protonated species resulting from the hydrolysis products.

Table 2: FT-IR spectrum analysis of *Sida acuta* extract

Wavenumbers cm^{-1}	Band characteristics	Functional groups	Heteroatoms
3380	Broad and strong	Phenol, O-H	Oxygen, O
2925	Strong	Carboxylic acid O-H	Oxygen, O
2854	Weak	Aldehyde C-H	-
1711	Stretching	Carbonyl C=O	Oxygen, O
1620	Strong	Amines or Oximes C=N	Nitrogen, N
1257	Weak	Alcohol,ether, ester,C-O-	Oxygen, O
1057	Strong	Alcohol, ether, ester, C-O-	Oxygen, O

Table 3: FT-IR Spectrum analysis of *Jatropha curcas* extract

Wavenumbers cm^{-1}	Band characteristics	Functional groups	Heteroatoms
3420	Broad and Strong	Phenol, O-H	Oxygen, O
2922	Strong	Aliphatic C-H	-
2852	Weak	Aliphatic C-H	-
1663	Strong	Ketone, C=O	Oxygen, O
1458, 1404, 1378	Weak	Nitro, N=O-	Nitrogen, O
1054	Stretching vibration	Alcohol, Ether, Ester C=O	Oxygen, O
719	Weak	Amines, C=N-	Oxygen, O

Table 4: FT-IR Spectrum analysis of mixed extract of *Sida acuta* and *Jatropha curcas*

| Wavenumbers cm^{-1}	Band characteristics	Functional groups	Heteroatoms
3381	Broad and weak	Carboxylic, O-H	Oxygen, O
3012	Stretching vibration	Aromatic C-H	-
2853	Weak	Aliphatic, C-H	-
1744*	Strong	Ester or Lactone, C=O	Oxygen, O
1644	Weak	Imines and Oximes C-N	Nitrogen, N
1463 and 1376	Weak	Nitro, -N=O	Nitrogen, N and Oxygen, O
1240, 1162, 1094	Stretching vibration	Alcohol, Ether,Ester C-O-	Oxygen, O
724 and 661	Bending vibration	Amines, C=N	Nitrogen, N
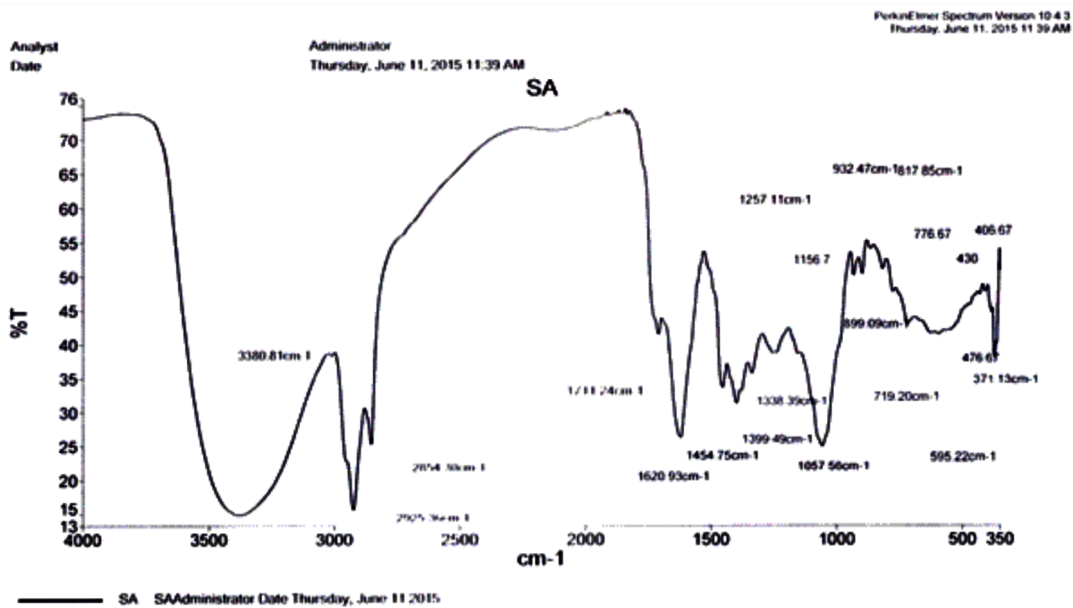
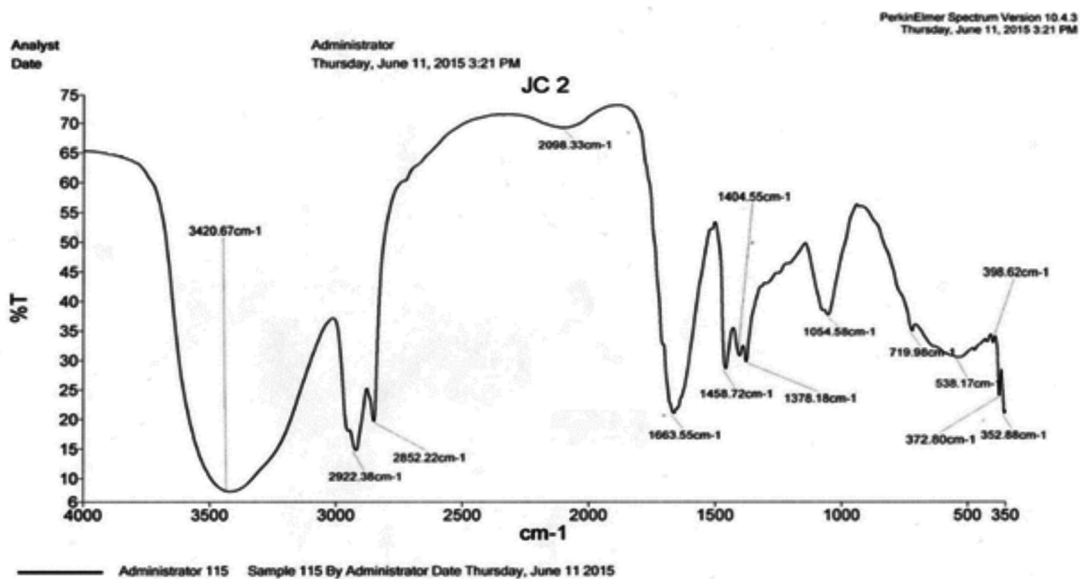**Fig. 6** FTIR Spectrum of *Sida acuta* leaf extract.

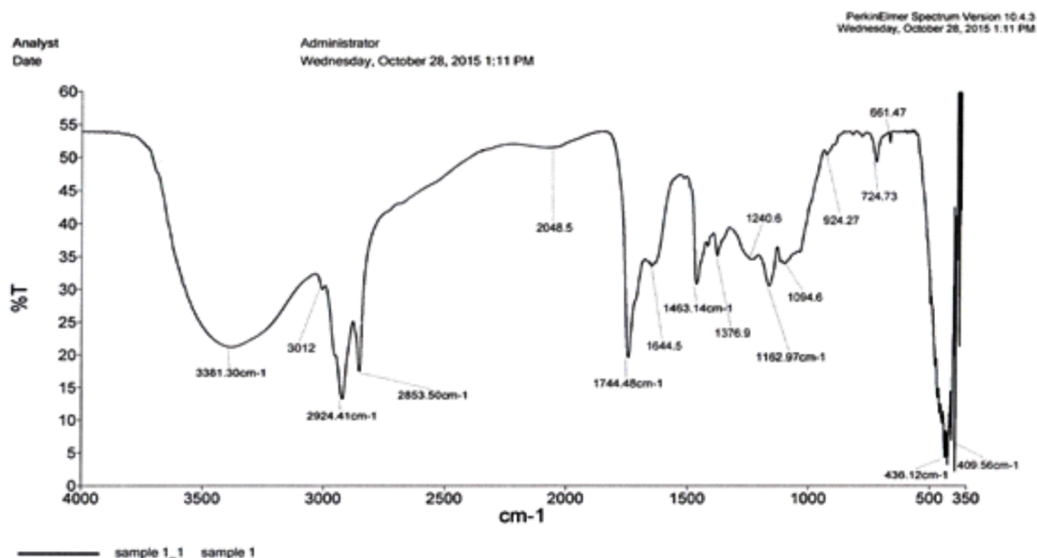**Fig. 7** FTIR Spectrum of *Jatropha curcas* leaf extract.

Fig. 8 FTIR Spectrum of mixture of *Sida acuta* leaf with *Jatropha curcas* leaf extracts

3.4 Microstructural Studies of Coupons

The SEM and EDX micrograph of the mild steel coupons (inhibited and uninhibited) are shown in Fig. 9 and 10 respectively. In Fig. 9a there is the presence of a protective layer due to the mixed extract over the structrure of the steel. This hindered the attack of acid on the microstructures thus prevented dissolution of some constituents into corrodent to some extent. As shown in Fig. 9b, much of the a-Fe phase dissolved into the acid solution, this is due to the aggressive effect of the acid on the steel surface down into deep internal structure.

There was also erosion of the ferrite phase with most of the surface covered by pearlite. The EDX spectrum of the inhibited coupon (Fig. 10a) showed prominent iron peak, as base material to depict reduction in lost of material due to inhibitory effect of the extract. with the high value of 78.06 % Iron, low value of 6.22 % carbon and 15.71 % Oxygen. Fig 10b shows promient peak of Iron and of impuirities such as zirconium with oxygen and carbon. The low value of 61.49 % Fe and high value 33.38 % of Oxygen was an indication of high activities of corrosion on steel caused by the acid without extract.
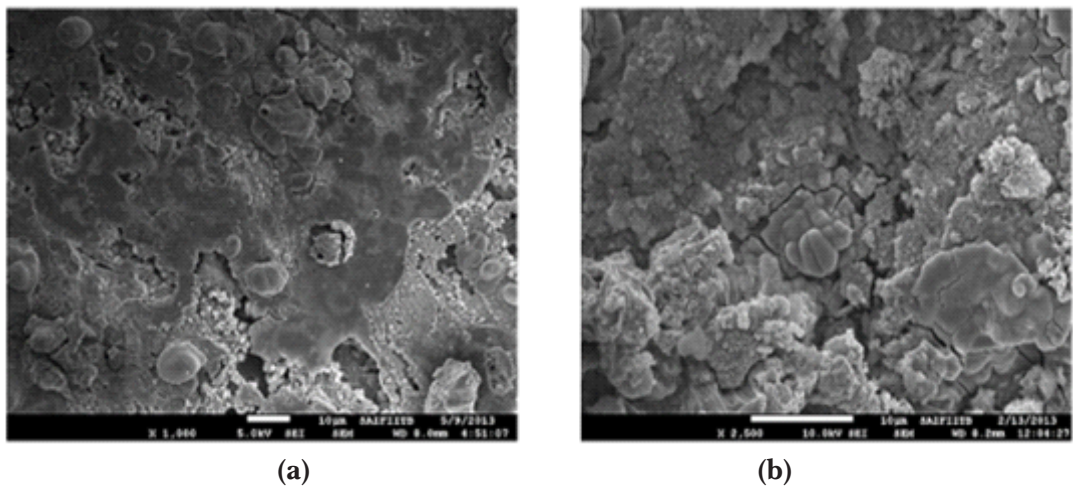
(a)   **(b)**

Fig. 9 (a) SEM spectrum of protected steel in *Synergized* extract (b) SEM spectrum of steel in 1.0M HCl (Control)
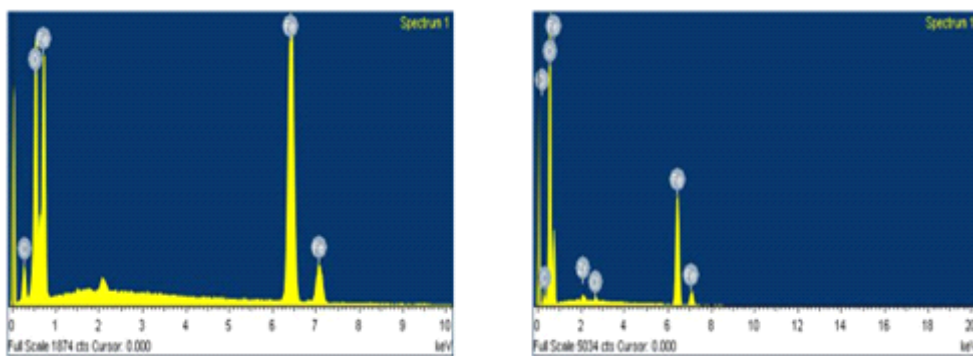

Fig 10. (a) EDX Spectrum of protected steel in *Synergized* extract (b) SEM spectrum of steel in 1.0M HCl (Control)
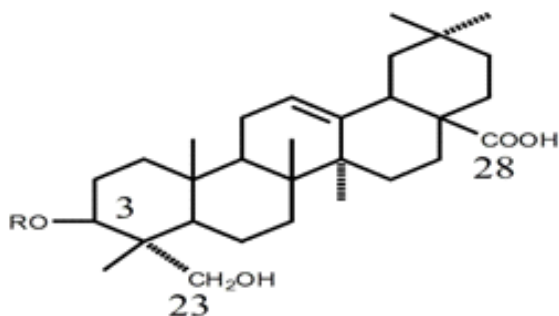

Fig. 11 Structure of Oleanane type Saponin (Yukiyoshi *et al.,* 2012)

Saponin as one of the phyto-constituents present in the two extracts that was synergized. It is a terpenoid with the structure shown in Fig. 8, having both COOH of acid and OH of alcohol functional groups at position 28 and 23 respectively. There could have been an intermolecular esterification occurrence between the COOH of saponin from the first plant with that of OH alcohol of the second plant extracts. This reaction is aided or catalysed by the presence of mineral acidic medium. When this happened, there is disappearance of both COOH and OH, an alkoxycarbonyl (of ester presence) thus appeared. This will alter the rate and manner of foaming in the resulted solution that could have been expected for a normal saponin. This intermolecular esterification also explain why saponin is positive in both JC and SA leave extracts but absence (-ve) in the mixture of spent or unused (see Table 1).

Acid catalysed esterification process is an equilibrium-controlled reaction. However, in the combination of the two extracts, there was no more 28-COOH and 23-OH, which signified that the equilibrium tilted to the right to form ester. Esters are moderately polar; possibly have δ^+ and δ^- on carbonyl carbon and oxygen. It can also be protonated in the acidic media, as products of the reactions was not isolated from the system (Carey, 2003). The δ^- end of the newly formed specie may be attracted to the surface of metal. The remaining phyto-constituent in solution such as saponins leftover attained equilibrium and other secondary metabolites that did not partake in the intermolecular reactions but contains heteratoms having lone pairs of electrons that could be attracted to the end of δ^+ of the ester. The ester can form bond with the metal through the lone pair of electrons from carbonyl oxygen and alkoxyl oxygen in a chelating structure.

The adsorption resulted from this chelating structure is compare to that formed from extracts synergized with halides that employ electrostatics attractions to improve adsorption of leave extracts on metals (Larabi *et al.*, 2004). Furthermore esters can also function as a Lewis base due to lone pair of electrons on its carbonyl and alkoxyl oxygen atoms which forms dative covalent bond with the metal. It is worth noting that carbonyl is a very strong field ligand which stabilizes the Fe^{2+}, as the low spin Fe^{2+}, with t_2g_6 configuration which stabilizes the iron Fe^{2+} against corrosion or oxidation to Fe^{3+}. This probably explains the extracts better inhibitory activities. The carbonyl oxygen of the ester can also be protonated in the acidic solution. Through this protonated carbonyl oxygen, adsorption could occur at the cathodic sites to hinder release of hydrogen gas as a product of corrosion reaction. This however contributed to the synergistic characteristics of the mixture.

3.5 Adsorption Studies of Synergised Extracts on the Steel

Adsorption studies reveal how the adsorbed molecules interact with each other and on the metal surface. The chemical properties of the inhibitor, the configuration of electronics therein and the nature of the inhibitor determine the manner of adsorption (physio or chemisorptions) (Aladesuyi *et al*., 2019; Sodiya *et al*., 2016). Adsorption also plays a major role in understanding the behaviour of non-homogenous organo-electrochemical reactions involving solid surfaces (Aladesuyi *et al*., 2019). For equations deduced from graphs on Figure 12,

$$y = 1.0477 \, x + 0.0438 \text{ at } 30 \,^{\circ}\text{C} \tag{12}$$

$$\text{and} \quad y = 1.2161 \, x + 0.0993 \text{ at } 50 \,^{\circ}\text{C}, \tag{13}$$

considering Lagmuir adsorption isotherm equation $q = KC/[1+kc]$

Plot of a linear graph C/q against Concentration C, $1/k = 0.0438$, k = 22.83 at 30 oC. Also $1/k = 0.0993$, k = 10.07 at 50 $^{\circ}$C shows favourabilty of adsorption to Langmuir adsorption isotherm with Coefficient of determination $R^2 = 0.996$ and Correlation coefficient R = 0.998 at 30 $^{\circ}$C and $R^2 = 0.988$, R = 0.994 at 50 $^{\circ}$C.
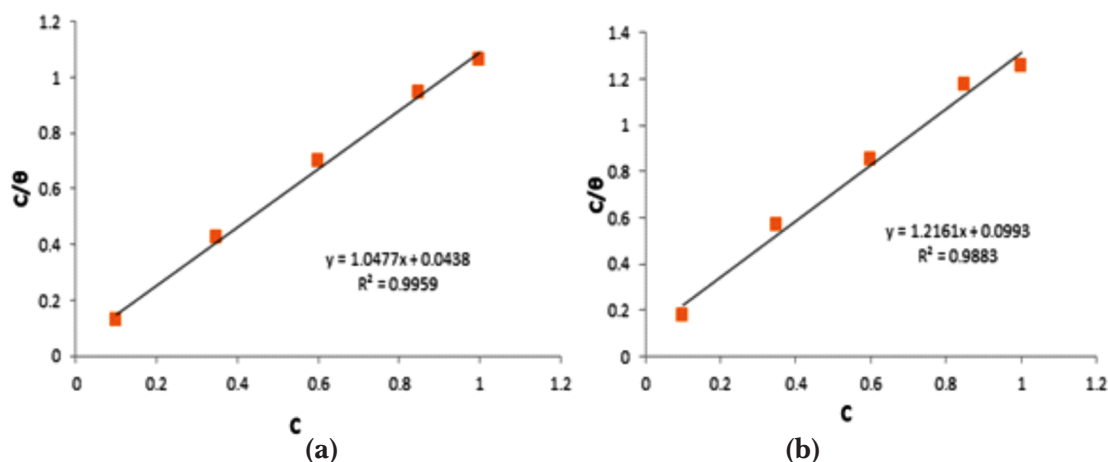

Fig. 12: Plot of Concentration C of Synergized extracts against C/θ showing agreement with Langmuir isotherm for steel in the presence of 1.0 M HCl at (a) 30 $^{\circ}$C and (b) 50 $^{\circ}$C

4.0 Conclusion

Synergism Parameter S_1 greater than 1 with increase in temperature confirmed that the mixture of the two plants yielded synergistic effect by improved Inhibition efficiencies of synergised over unsynergized. The SEM micrograph of the steel coupons indicated presence of a protective layer due to the mixed extract over the structrure of the steel. This hindered the corrosive process on the microstructures thus improved the prevention of metal constituent's dissolution into corrodent. The EDX correspondingly confirmed with the high value of 78.06 % Iron, low value of 6.22 % carbon and 15.71 % Oxygen as against low value of 61.49 % Fe and high value 33.38 % of Oxygen shows the effect of the acid without extract with high activities of corrosion on steel. This is obtained due to improved potency of the heteroatoms present responsible for the corrosion inhibition. Inhibition Efficiency ranges from 60 % to 85 % with increase in extract concentration of SA alone from 0.1 gdm^{-3} to 1.0 gdm^{-3}. When synergised with JC, it ranges from 77 % to 93 % for SA at 30 $^{\circ}$C for the same concentration increase. Therefore the synergetic effects of the plants extracts complimented carbon constituent of the steel to enhanced the corrosion inhibition potential synergized plant extracts over unsynergized on the steel.

References

Ajanaku, K.O., Ajanaku, C.O., Akinsiku, A.A., Falomo, A., Edobor-Osoh, A. and John, O.M. (2014). Eco-friendly impact of *Vernonia amygdalina* as corrosion inhibitor on Aluminium in Acidic Media. *Chemistry Journal*, 2(4):153 - 157.

Ajayi, O.O., Omotosho, O.A., Ajanaku, K.O. and Olawore, B.O. (2011). Failure evaluation of Aluminium alloy in 2.0 M Hydrochloric acid in the presence of *Cola acuminate*. *Journal of Engineering and Applied Sciences*, 6(1):10 - 17.

Aladesuyi O., Ajanaku K.O., Badejo A.V., Ademosun O.T. and Ajayi O.S. (2019). Corrosion inhibitive properties of *Epimedum grandiflorum* on Mild steel in HCl Acidic media. *IOP Conference Series: Material Science and Engineering*, 509(1):102008 doi:10.1088/1757-899X/509/1/012008

Aramaki, K., & Hackerman, N. (1969). *Inhibition Mechanism of Medium-Sized Polymethyleneimine. Journal of The Electrochemical Society*, 116(5), *568*. doi:10.1149/1.2411965

Ating, E.I. Umoren, S.A. Udousoro, I.I. Ebenso, E.E. and Udoh A.P. (2010). Leaves Extract of *Ananassativum* as Green Corrosion inhibitor for Aluminium in Hydrochloric acid solutions. *Green Chemistry Letters and reviews*, 3:2, 61-68, DOI: 10.1080/1751825 0903505253

Fishtik, I.F., Vatman , I.I. and. Spatar F. A (1984). The Mechanism of ion-pair formation in the inner part of the double layer. *Journal of Electroanalytical Chemistry*, 165(1-2):1–8.

Ita, B, I and Effiong, O. E (2000). Inhibition of Mild steel corrosion in HCl by 2- Aminopyridine and 2- (Aminomethyl) Pyridine. *Global Journal of Pure and Applied Sciences,* 6(1):51-53.

Kumari, P.P., Shetty, P. and Rao, S.A. (2020). Synthesis, Characterization and Anticorrosion behaviour of a novel Hydrazide derivative on Mild steel in Hydrochloric acid Medium. *Bulletin Mater Sci.*, 43(46): doi:10.1007/s12034-019-1995-x

Larabi, L., Harek, Y., Traisnel, M., Mansri, A., (2004). Synegistic effect of poly (4-vinylpyridine) and potassium Iodide on Inhibition of corrosion in Mild steel in 1.0 M HCl. *Journal of Applied Electrochemistry*, 34:833-839

Mamatha, G. P., Pruthviraj, R. D. and Ashok, S. D. (2011). *International Journal of Researching Chemistry and Environment,* 1: 85 - 88.

Mathur, P. B. and Vasudevan, T. 1982. Reactions Rate studies for the corrosion of metals in acid - I Iron in mineral acids Corrosion. National Association of Corrosion Engineers. (NACE) 38(3):171 – 178.

Noor, E. A. (2005). The inhibition of mild steel corrosion in phosphoric acid solutions by some N- heterocyclic compounds in the salt form Corrosion Science, 1(47): 33.

Nwabanne, J. T., Okafor, V. N. and Chima, L. O. (2011). Adsorption mechanism and synergistic inhibitive effect of *Telfairia occidentalis* for the corrosion of mild steel in HCl. *Journal of Engineering and Applied Sciences*, 3: 92 – 100.

Obot, I.B., Umoren, S.A. and Egbedi, N.O. (2011). Corrosion inhibition and Adsorption behavior for Aluminium for extract of *Aningeria robusta* in HCl solution: Synergistic effect of iodide ions. *Journal of Material Environmental Science*, 2(1): 60 - 71.

Obot, I. B. and Obi-Egbedi, N. O. 2009. *Impomoea Involcrata* as an Ecofriendly Inhibitor for Aluminium in Alkaline medium. *Portugaliae Electrochimica Acta*, 27(4): 517 - 524.

Oguzie, E. E. (2006). Studies on the inhibitive effect of *Occimum Viridis* extract on the acid corrosion of mild steel. *Material Chemistry and Physics*, 99 (2/3): 441 – 446.

Oguzie, E. E. (2008). Corrosion Inhibitive effect and Adsorption behaviour of *Hibiscus Sabdariffa* extract on Mild steel in acid media. *Portugaliae Electrochimica Acta*, 26: 303 – 314.

Omotosho, O.A., Ajayi, O.O., Ajanaku, K.O. and Ifepe, V.O. (2012). Environmental induced failure of Mild steel in 2.0 M Sulphuric acid using *Chromolaena odorata*, *Journal Material Environmental Science*, 3: 66 - 75

Orubite, O.K. and Oforka, N. C. (2004). Inhibition of the corrosion of mild steel in HCl solution by the extracts of *Nypa fruticans Wumb*. *Materials Letters*, 58 (11): 1768 – 72.

Orubite-Okorosaye, K., Oforka, N.C. 2004. Corrosion Inhibition of Zinc on HCl using *Nypa fruticans Wurmb* Extract and 1,5 Diphenyl Carbazone. *Journal of Applied Science and Environs Mgt.*, 8(1): 56.

Sodiya E. F., Dawodu F. A., Oyedele A. A. (2016). Synergized Plant Leave Extracts as Substitute to Toxic Additives in Alkyd Resin Primer for Corrosion Inhibition of Steel. *American Journal of Applied Chemistry*, 4(3): 97-103.

Umoren, S.A., Obot, I.B. and Ebenso, E.E. (2008). Corrosion inhibition using exudates gum from *Phachylobus edulis* in the presence of halide ions in HCl. *e-Journal of Chemistry*, (5):355-364.

Yukiyoshi, T., Masazumi, M. and Masaji, Y. (2012). Application of Saponin Containing Plants in Foods and Cosmetics. Alternative Medicine 7: 306. ISBN 978-953-51-0903- InTech, Chaptershttp://dx.doi.org/10.5772/53333.

Zhao, H. Duan and Jiang R. (2015). Synergistic corrosion inhibition effect of Quinoline quaternary ammonium salt and Gemini surfactant in H_2S and CO_2 Saturated brine solution. *Corrosion*